



OPEN

A new approach for determination of orthophosphate based on mixed valent molybdenum oxide/poly 1,2-diaminoanthraquinone in seawater

Mahmoud Fatehy Altahan^{1✉} & Magdi AbdelAzzem²

Orthophosphate is an essential macronutrient in natural water that controls primary production and strongly influences the global ocean carbon cycle. Electrochemical determination of orthophosphate is highly recommended because electrochemistry provides the simplest means of determination. Here the determination of orthophosphate based on the formation of a phosphomolybdate complex is reported. Mixed-valent molybdenum oxide (Mo_xO_y) was prepared by cyclic voltammetry on poly-1,2-diaminoanthraquinone (1,2-DAAQ), which was performed by cyclic voltammetry on the surface of a glassy carbon electrode under pre-optimized conditions for the thickness of the modified electrode layers. The proposed modified electrode was used for square-wave voltammetry of orthophosphate ions under pre-optimized square-wave parameters (i.e., frequency and amplitude) in strongly acidic medium ($\text{pH} < 1$). The linear range was 0.05–4 μM with a limit of quantification (LOD) of 0.0093 μM with no effect on two peaks due to cross interference from silicate. Furthermore, $\text{Mo}_x\text{O}_y/\text{PDAAQ}$ shows good reproducibility with a relative standard deviation (RSD) of 2.17% for the peak at 0.035 V and 3.56% for the peak at 0.2 V. Real seawater samples were also analyzed for PO_4^{3-} analysis by UV spectrophotometry and the results were compared with the measurement results of our proposed electrode, with good recoveries obtained.

Phosphate is considered as an essential chemical compound in the body's cells. Phosphate plays an important role as a building block for phospholipids, nucleic acid, and adenosine triphosphate (ATP). Those biomolecules play an important role in the storage or utilization of genetic information^{1,2}. However, when excessively accumulated, phosphate can cause many serious social problems, which are reflected in its strong environmental and health effects³. In the environment, phosphorus can be occurred in different chemical forms, which can be classified as follows: inorganic phosphates such as orthophosphate (PO_4^{3-}), which is considered the usual soluble form of phosphate. Other condensed phosphate forms are pyro- ($\text{P}_2\text{O}_7^{4-}$), meta- (PO_4^{3-}) and polyphosphates ($[\text{PO}_4^{3-}]_n$) and the second form is organic phosphates⁴. Most of the inorganic phosphates are contained either in agricultural fertilizers or in food. Those phosphate forms enter the environment and lead to eutrophication of surface waters. Those are causing extreme production of biological material (mainly algae) and throttling of aquatic ecology⁵. In addition, excess or deficiency of phosphate can cause many serious human diseases such as hypophosphatemia (phosphate deficiency) and hyperphosphatemia (phosphate excess)⁶.

It is obvious that a highly sensitive, stable, and safe determination tool is needed for continuous monitoring of phosphate to detect its environmental and health effects. For example, the colorimetric method is still the recommended standard method for measuring phosphate in water. The method incorporated molybdenum ions which are complexed using antimony tartrate ($\text{C}_{12}\text{H}_{12}\text{O}_{18}\text{Sb}_2$) and ascorbic acid as reducing agents to form yellow or blue phosphomolybdate $[\text{PMo}_{12}\text{O}_{40}]^{3-}$ or $[\text{PMo}_{12}\text{O}_{40}]^{4-}$, respectively⁷. This method, based on enormous reagents, is time consuming and cannot be used for on-line measurements. Alternative analytical techniques for phosphate detection have been developed, such as ion chromatography (IC), luminescence/fluorescence

¹Central Laboratory for Environmental Quality Monitoring, National Water Research Center, El-Qanater El-Khairia 13621, Egypt. ²Electrochemistry Laboratory, Chemistry Department, Faculty of Science, Menoufia University, Shibin El-Kom 32511, Egypt. ✉email: mahmoud_abdalqader@nwrc.gov.eg

sensors, and biosensor⁸. Nevertheless, electrochemical determination methods have already been developed using mobile devices⁹.

Electroanalytical methods developed for the determination of phosphate offer many advantages such as rapidity, cost efficiency, and lack of intervention due to sample turbidity. In the last decades, many potentiometric ion-selective electrodes (PISE) have been developed based on either a metal, organic complexes or metal complexes⁸. Various forms of PISE have been investigated, with metal-based PISE such as silver phosphate sensors suffering from interference from chloride ions¹⁰. PISE of organic complexes such as organic tin compounds (IV)¹¹, PISE of cobalt using a cobalt phosphate/Co electrode¹², PISE of metal complexes such as Zn (II) complexes¹³, and finally PISE of polymers such as polyaniline/gold electrodes¹⁴. These PISE have good lifetime; however, the sensitivity is different due to some interferences that require subsequent calibration before use. Polyvinyl chloride (PVC)-based bis(dibromophenylstannyl)methane, which detects only HPO_4^{2-} and other inorganic phosphates¹⁵. These PISE have not been tested in surface or contaminated water. Other voltammetric sensors developed for the determination of phosphate in water use cyclic voltammetry (CV)¹⁶, which is not suitable for rare nanomolar phosphate concentrations. Pulsed techniques such as differential pulse voltammetry (DPV), which has a detection limit of $0.19 \mu\text{M}$ ¹⁷, but has some difficulties due to the complicated optimization of DPV parameters and lack of repeatability.

Another type of pulsed technique, square wave voltammetry, shows better performance compared to DPV. Square wave voltammetry was first used by Barus, using an Au electrode as the working electrode and a Mo electrode to electrolyze molybdate. A LoD of $0.05 \mu\text{M}$ was obtained¹⁸.

Recent work has been published on the determination of phosphate on molybdate/carbon paste electrode pretreated with Sodium chloride solution and used for square wave voltammetry of orthophosphate¹⁹. The application of the proposed method was also reported into a prototype based on the Bi-potentiostat technique into flow injection analysis²⁰.

In this article, for the first time Mo in the form of molybdenum oxide is reported, which was previously prepared by Tian et al.²¹ and applied to poly 1,2-diaminoanthraquinone. Poly 1,2-diaminoanthraquinone along with other isomers were previously prepared by our group^{22–25}. This work could help achieve our investment goal and anticipated goals of expanding the use of on-site sensors to assess water quality²⁶.

This electrode is used as a fast electrochemical sensor for direct square-wave voltammetry of phosphate ions. The electrochemical measurement was performed without additives under acidic conditions. A very low detection limit with good repeatability was obtained. Good recoveries were obtained when real seawater samples were analyzed using classical spectrophotometric methods.

Results and discussion

Preparation of modified electrode. The anodic polymerization of DAAQ using cyclic voltammetry (Fig. 4A) was described earlier in our previous work. The cyclic voltammogram shows three primary peaks. The first primary peak is at 0.9 V, with the peak current decreasing as the number of sampling cycles increases. This peak relates to the consumption of the monomer molecules as polymerization proceeds. The other two peaks relate to polymer formation. The first peak is at 0.5 V, where the peak current increases with increasing sampling cycles. This peak represents the reduction of the monomer DAAQ to the radical anion form. The second peak, which occurs at 0.55 V, corresponds to the oxidation of the radical DAAQ anion to the dimeric state. The introduction of those substances increases the surface area of the electrode and increases the accessibility of the electrolyte to the active sites of the electrode. In the literature cyclic voltammetry is the technique used to form molybdenum oxide on the electrode surface because of the nature of the technique for consecutive oxidation and reduction steps. The formation of molybdenum oxide mixed valent (Mo_xO_y) was performed using cyclic voltammetry as shown in Fig. 4B. The figure shows that the highest reduction peak at -0.48 V in the first scan cycle is due to the deposition of the reduced molybdenum species on the electrode surface. The peak corresponds to the reduction of Mo (VI) to Mo (V) and Mo (IV) supports the formation of the polymeric layer of the oxide film with mixed valence of Mo (VI) and Mo (V), while the number of scan cycles increases. The cathodic peak current decreased because of already formed oxide film on the electrode surface. There is a low significant anodic peak at -0.22 V may be due to the oxidation of Mo (IV) to Mo (V) during the oxide film formation.

Square wave voltammetry of PO_4^{3-} on Mo_xO_y /PDAAQ modified electrode. Determination of phosphate ion in sea water performed using SWV at different electrode for $10 \times 10^{-6} \text{ M}$ PO_4^{3-} (Fig. 1) firstly at glassy carbon, there is not any peak indicating the presence of phosphate ion into the solution, while with using Mo oxide film there are two clearly peaks at 0.02 V and 0.12 V are due to the gradual oxidation of Mo (II) to Mo (IV) and Mo (IV) to Mo (VI), respectively. For using the PDAAQ film, there is not any significant peak. However, at Mo_xO_y /PDAAQ modified electrode, two high peaks obtained at -0.035 V and 0.2 mV with about 3 and 2 times, respectively, higher than that obtained at Mo_xO_y /GC electrode. For the results obtained, the MoO_3 /PDAAQ/GC is considered the perfect electrode to detect phosphate in sea water.

Optimization of preparation parameters. One of the key parameters that has a significant impact on the performance of the conducting polymer or the metal oxides that were formed by cyclic voltammetry is the thickness of the thin film or surface layer being exhibited. The thickness of the layer of the film is investigated by the number of scanning cycles of the cyclic voltammetry. The thickness of the polymer or metal oxide film is increasing with increasing the number of scanning cycles.

The effect of thickness of polymer film on the peak currents of both peaks at -0.015 V and 0.185 V studied depending on the number of scanning cycles during polymer formation as the concentration of the monomer remains constant during film fabrication. A solution of $10 \mu\text{M}$ PO_4^{3-} into 30 g L^{-1} NaCl was tested with the

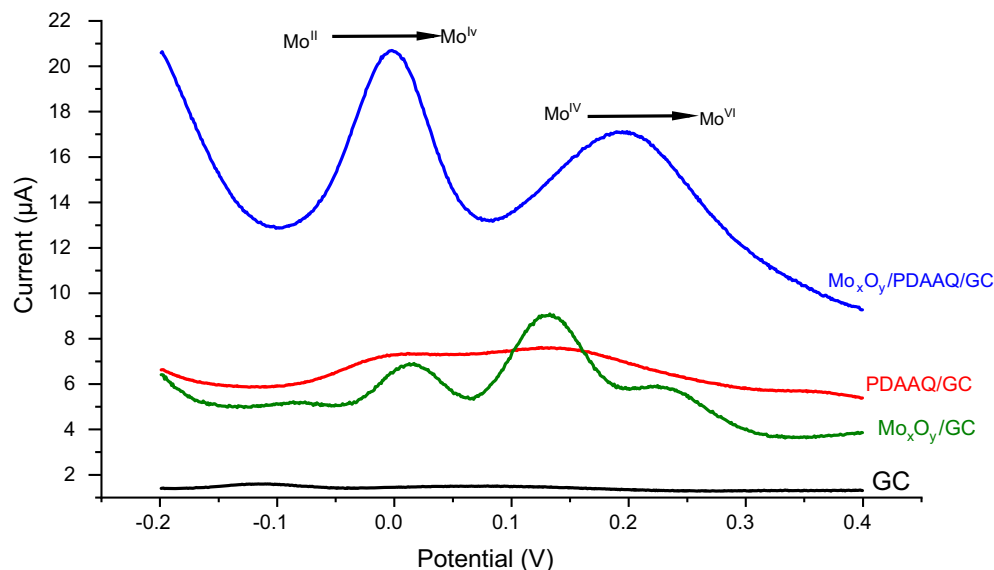


Figure 1. Square-wave voltammograms of $10 \mu\text{M PO}_4^{3-}$ in a solution of artificial seawater (34.5 g/L) pH 1 with a potential range of -0.2 to 0.4 V with a step potential of 1 mV, an amplitude of 25 mV and a frequency of 100 Hz on a glassy carbon electrode without any modification (black line), a glass carbon electrode after modification by a layer of mixed-valency molybdate oxide (green line), a glassy carbon electrode modified by a layer of poly-1,2-diaminoanthraquinone (red line) and a glassy carbon electrode modified by a layer of mixed-valent molybdate oxide and poly-1,2-diaminoanthraquinone (blue line).

number of scanning cycles varied from 2 to 15 cycles with 10 scanning cycles of molybdenum oxide. The results show that polymer film formed with 5 cycles is the best polymer film formed at which the highest peak current of $5 \mu\text{A}$ and $3 \mu\text{A}$ at -0.015 V and 0.185 V are reported, respectively.

Also, the effect of the thickness of the Mo oxide film on the peak currents of the two peaks corresponding to both Mo (II) to Mo (IV) and Mo (IV) to Mo (VI), respectively, studied from 5 to 20 cycles showing that the increase in peak currents of the two peaks while increasing from 5 to 10 scanning cycles while with raising above 10 cycles, there is a steady state in the quantity of the peaks current of about $5.5 \mu\text{A}$, $3.2 \mu\text{A}$ at -0.015 V, 0.185 V, so that 10 scanning cycles is the preferred preparation condition in forming the oxide film electrode.

Analytical performance of phosphate ion @ $\text{Mo}_x\text{O}_y/\text{PDAAQ}/\text{GC}$ electrode. A series of concentrations of phosphate ion in solution containing NaCl (34.5 g/L) as a simulated sea water used to study the analytical performance of the modified electrode ($\text{Mo}_x\text{O}_y/\text{PDAAQ}/\text{GC}$ electrode) as shown in Fig. 2, where phosphate ion concentrations varied from 0.03 to $4 \mu\text{M}$ showing a perfect gradual increasing in the peak current in accordance with raising the phosphate concentration and this clearly represented in the good linearity of the calibration plot of the current recorded at 0.015 V (while at $E=0.2$ V, there is a lower value of R^2 ; linearity of calibration curve) vs. the phosphate concentration with coefficient of detection $R^2=0.9956$ and regression equation $I (\mu\text{A})=0.711 C_{\text{PO}_4^{3-}} (\mu\text{M})+0.8929$. However, with increasing the phosphate ion concentrations, there is an observed positive shift in the peak potential that could be due to the IR drop. While the LOD and the LOQ values are $0.0093 \mu\text{M}$ and $0.03 \mu\text{M}$, respectively, which calculated using the following equations:

$$\text{LOD} = 3 \times \text{SD}/S \quad (1)$$

$$\text{LOQ} = 10 \times \text{SD}/S \quad (2)$$

where SD is the standard deviation of 10 blank responses in a solution containing only NaCl, and S is the sensitivity of the calibration curve or by another means it is the slope of the curve.

In addition, the effect of presence of some cross interferences such as silicates, ammonium, chlorides, and sulphate which usually present in real water samples were tested without any significant change in the two phosphate related peaks ($\Delta E_p > 1\%$).

Table 1 shows comparison between our state-of-the-art modified electrode and literature published modified electrode. Our modified electrode displayed superior performance for electrochemical determination of orthophosphate in the last decade, with a highly sensitive detection limit. Additionally, our method presented a simple assay compared to other published articles.

The detection of orthophosphate in seawater is crucial for understanding nutrient cycling and eutrophication processes. Various analytical methods for the detection of orthophosphate in seawater have been published in the literature, including capillary electrophoresis, photometry, spectrophotometry, ion chromatography, and others. To investigate the effectiveness of our approach, we compared it with these existing methods using Table 2. The results show that our approach outperforms the other analytical techniques in terms of the linear range, which

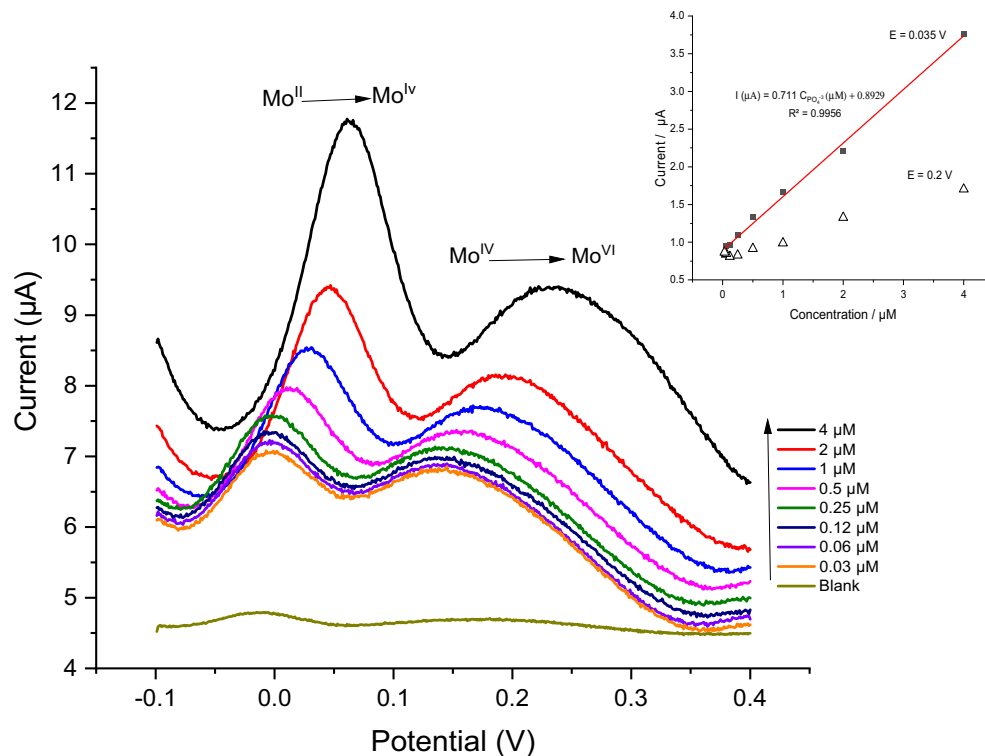


Figure 2. SWV of PO_4^{3-} recorded at $\text{Mo}_x\text{O}_y/\text{PDAAQ}/\text{GC}$ electrode under step potential 1 mV, amplitude 25 mV and frequency 100 Hz between -0.1 to 0.4 V in a solution of 34.5 g/L NaCl containing phosphate ion with a concentration from 0.03 to 4 μM and the inset is the calibration curve of the current recorded at $E = 0.015$ V/ Ag/AgCl vs. phosphate concentrations.

Electrode	Technique	Linear range (μM)	LoD (μM)	References
Mb rod ^a	Potentiometry (ISE ^b)	10–100	1.9	27
PANI ^c	Potentiometry (ISE)	1–100	1	14
Bis(DBPS)methane/PVC ^d	Potentiometry (ISME ^e)	$0.5\text{--}5 \times 10^3$	0.5	15
Chitosan-clay/PVC	Potentiometry	$1\text{--}1 \times 10^4$	0.6	28
CB-SPE-FIA ^g	Amperometry	1–80	0.1	29
CB/SPE	Amperometry	0.5–100	0.1	30
AuNWs ^h	Amperometry	$12.5\text{--}1 \times 10^3$	0.1	31
AuNWs/Pt	Amperometry	$48\text{--}1.4 \times 10^3$	45	32
Co(H_2PO_4) ₂ /Co	Amperometry	$0.1 \times 10^6\text{--}10 \times 10^6$	Not detected	33
Au electrode	DPV ⁱ	$0.65 \times 10^6\text{--}3.01 \times 10^6$	0.19×10^6	17
Au electrode	SWV ^j	0.1–1	0.05	18
$\text{Mo}_x\text{O}_y/\text{PDAAQ}/\text{GC}$	SWV	0.03–4	0.009	This study

Table 1. Electrochemical determination of PO_4^{3-} at different electrodes. ^aMb molybdate, ^bISE ion-selective electrode, ^cPANI polyaniline, ^dBis(DBPS)methane/PVC Bis (dibromophenylstannyl) methane/polyvinyl chloride, ^eISME ion-selective microelectrode, ^gCB-SPE-FIA carbon black nanoparticles-screen printed electrode-flow injection analysis, ^hAuNWs gold nanowires, ⁱDPV differential pulse voltammetry, ^jSWV square wave voltammetry.

is the typical range of orthophosphate content in seawater. Our approach showed excellent performance over the entire range of orthophosphate content, ranging from a few nanomolar in oligotrophic seawater to 3 μM in estuarine waters. This shows that our approach is very sensitive and accurate in detecting orthophosphate in seawater and provides researchers with a powerful tool to study environmental processes. Consequently, this study opens new possibilities for the detection of orthophosphate in seawater, expanding our understanding of nutrient cycling and eutrophication processes, and ultimately contributing to sustainable ocean management.

Analytical methods	Linear range (μM)	LOD (μM)	References
Capillary electrophoresis (CE)	0.5–10	0.45	34
Photometric	4.8–100	0.64	35
Spectrophotometry (blue method assay)*	0.14–10	0.04	36
Spectrophotometry (yellow method assay)*	0.1–60	0.052	37
Ion Chromatography (IC)	1.6–806	0.76	38
Square wave voltammetry ($\text{Mo}_x\text{O}_y/\text{PDAAQ}/\text{GC}$)	0.03–4	0.009	This study

Table 2. Comparison between analytical methods for determination of orthophosphate. *The methods were applied in microfluidic Lab on Chip.

Repeatability of modified electrode. Fifteen repetitive measurements of the same concentration of phosphate ion ($6 \times 10^{-6} \text{ M}$) at $\text{Mo}_x\text{O}_y/\text{PDAAQ}/\text{GC}$ electrode (Fig. 3) used to study the stability of the modified electrode during the repeated measurements without any significant deviation of the value of the peak current represented with RSD value of 2.17% and 3.54% and standard error (SE) of 0.035 and 0.026 for peak current at 0.035 V and 0.2 V, respectively, as shown in Fig. 3 providing the concept that our proposed method had a great advantage due to its stability during repetitive measurements.

Analysis of real sea water samples. Real saline water samples were collected off the coast of the Mediterranean Sea (Sample 1 and sample 2), certified reference materials (CRMs) termed as Reference Material for Nutrients in Seawater (RMNS). CRMs were purchased from KANSO TECHNOS CO., LTD with lot. Number CG, CI and CH. The assigned concentration of the collected samples and CRMs samples were mentioned in Table 3. Collected Samples measured by traditional colorimetric method using UV-visible spectrophotometer with the help of using Sb, ascorbic acid and in highly acidic medium ($5\text{N H}_2\text{SO}_4$). Also, the samples were analyzed with our proposed method ($\text{Mo}_x\text{O}_y/\text{PDAAQ}/\text{GC}$) electrode. Where the CRMs samples were analyzed as mentioned in certificates of Analysis (COA)^{39–41}. Good recovery values were obtained using our method comparing with this well-known method ranged from 93.5 to 107%. For 5 analyses for each sample, a paired t test with a degree of freedom (df) of 4 and a significance level of 1% was used to detect systematic error (bias) between those analyzed by our approach compare with those determined spectrophotometrically. No bias was found for the Mediterranean seawater sample 1 ($t\text{-value} = 0.55$, $t_{\text{critical (one-tail)}} = 3.747$, $p > 0.01$), the same

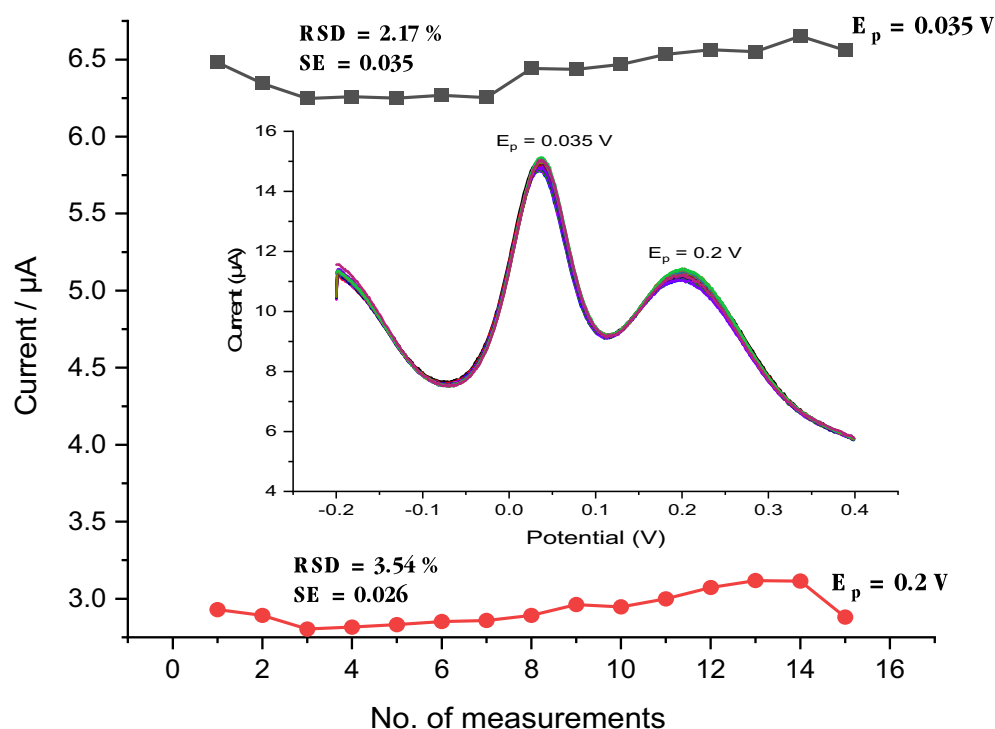


Figure 3. Peak current measurements of 15 repetitive measurements of $6 \times 10^{-6} \text{ M PO}_4^{3-}$ at ($\text{Mo}_x\text{O}_y/\text{PDAAQ}/\text{GC}$) electrode in solution containing 34.5 g/L NaCl for peak at 0.035 V and peak at 0.2 V and the inset represented the data gathered from every SWV response over 15 measurements.

	Sample type	Salinity/psu	Founded by UV-visible spectrophotometer $\pm \sigma^a$ (μM)	Founded by $\text{Mo}_x\text{O}_y/\text{PDAAQ}/\text{GC} \pm \sigma$ ($n^b=5$) (μM)	Recovery % vs. UV-visible spectrophotometer (%)
1	Mediterranean Sea sample 1	47.7	0.026 ± 0.005	0.0248 ± 0.004	95.4
2	Mediterranean Sea sample 2	52.3	0.025 ± 0.005	0.024 ± 0.005	94.5
3	Kanso CRM ^c CG	34.338	1.70 ± 0.0011	1.67 ± 0.174	98.23
4	Kanso CRM CI	35.654	0.948 ± 0.002	1.006 ± 0.02	106
5	Kanso CRM CH	34.991	1.172 ± 0.0016	1.144 ± 0.018	97.6

Table 3. Determination of PO_4^{3-} at UV-visible spectrophotometer and $\text{Mo}_x\text{O}_y/\text{PDAAQ}/\text{GC}$ electrode. ^a σ standard deviation, ^b n number of analyses, ^cCRM certified reference material.

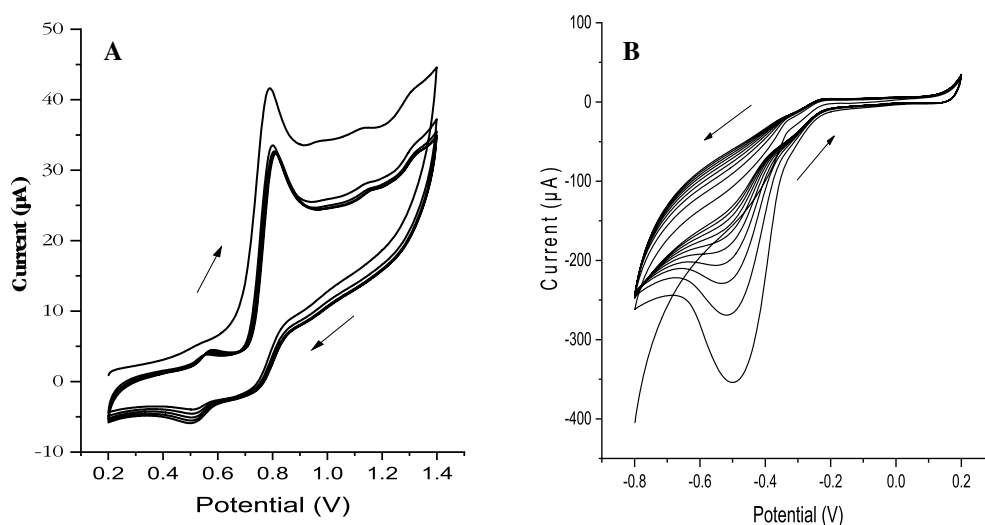


Figure 4. (A) Repetitive cyclic voltammograms of 1 mM DAAQ on glassy carbon electrode at a potential range from 0.2 to 1.4 V (vs. Ag/AgCl, 3 M KCl) at a scan rate of 0.1 V s^{-1} for five scanning cycles with increased peak current at an oxidation potential of 0.6 V and a reduction potential of 0.5 V. (B) Repetitive cyclic voltammograms of 5 mM ammonium molybdate tetrahydrate in a solution containing 50 mM Na_2SO_4 , pH 3 with a potential range from -0.8 to 0.2 V at a scan rate of 0.1 V s^{-1} for 10 scanning cycles with increased peak current at an oxidation potential of -0.2 V and at a reduction potential of -0.5 V.

is true for well water where there is no bias (t -value = 0.58, $t_{\text{critical (one-tail)}}$ value = 3.747, $p > 0.01$), it is true for Kanso CRM CG (t -value = 0.38, $t_{\text{critical (one-tail)}}$ value = 3.747, $p > 0.01$) and also for Kanso CRM CH (t -value = 3.44, $t_{\text{critical (one-tail)}}$ value = 3.747, $p > 0.01$), where there is no bias. On the other hand, significant differences were found between the values determined by our method and spectrophotometrically for Kanso CRM CI (t -value = 6.05, $t_{\text{critical (one-tail)}}$ value = 3.747, $p < 0.01$). In addition, the F-test was used to determine the bias between the analyses of the samples determined by our method and those determined by the reference colorimetric method. With df between groups ($df_1 = 1$) obtained as " $k-1$ ", where k is the number of groups equal to 2, and df_2 , which is the degree of freedom within the group with " $n-k$ ", where n is the total number of samples ($df_2 = 8$). The same results were obtained as for the t -test, where no bias was obtained for the Lake Burullus sample (F -value = 8.96, F_{critical} value = 11.259, $p > 0.01$), the same is true for the well water sample (F -value = 0.88, F_{critical} value = 11.259, $p > 0.01$) and it is also true for Kanso CRM CG (F -value = 0.15, F_{critical} value = 11.259, $p > 0.01$). Significant differences between the analyses of the samples by both methods exist for Kanso CRM CI (F -value = 35.7, F_{critical} value = 11.259, $p < 0.01$) and for Kanso CRM CH (F -value = 11.84, F_{critical} value = 11.259, $p < 0.01$). Overall, the analysis of real saltwater samples shows good values for three samples over 5 samples without bias observed as results of the t -test and f -test. For CRM CH, a recovery value of 97.6% above the mean values shows a good recovery value, while for CRM CI, a value of +2 above the accepted tolerance for the recovery values ($100 \pm 5\%$) could be accepted for our approach as a substitute for the traditional method that consumes many reagents.

Conclusion

Overall, preparation of a poly-1,2-diaminoanthraquinone on a glassy carbon electrode was succeeded. Ammonium molybdate was deposited on the modified electrode. The modified electrode was used for square wave voltammetry for orthophosphate in artificial seawater under acidic conditions. A typical voltammogram for orthophosphate is obtained with two oxidation peaks at 0 V and 0.2 V. Very good linearity was obtained with an R square value of 0.9956 for a linear range from 0.03 to $4 \mu\text{M}$ with a detection limit of $0.003 \mu\text{M}$. Good precision was obtained with an RSD value of 2.17% and 3.45% for peaks at 0.035 V and 0.2 V, respectively. Good recovery values for samples analyzed by our method compared to those measured by classical colorimetric methods. Our

future work will focus on the application of our method in a fully automated prototype for on-site analysis of orthophosphate in seawater.

Experimental

The poly-1,2-diaminoanthraquinone-modified electrode was prepared on a 3.0-mm-diameter glassy carbon (GC) electrode (Bioanalytical Systems, Inc. (BASi), USA). A three-electrode voltammetric cell was used, with the glassy carbon electrode as the working electrode and the silver/silver chloride reference electrode fed with 3 M potassium chloride (KCl, Merck, USA) (BASi, USA) and a platinum wire (BASi, USA) as the counter/auxiliary electrode. All voltammetric measurements were performed using an Epilson EC model potentiostat connected to a cell stand (BASi, U.S.). The glass carbon electrode was pre-washed with deionized water after being polished with a polishing set containing 0.3 μm aluminium suspension. The glass electrode was electrochemically cleaned by applying a fixed potential of 0.3 V into a solution of 0.1 M NaOH for 30 s with stirring at 400 ppm. The anodic polymerization of the 1,2-diaminoanthraquinone was done on glassy carbon followed by the polymerization of mixed valent oxide layer.

The modified electrode was prepared by cyclic voltammetry in a voltammetric cell containing 1 mM diaminoanthraquinone (DAAQ) ($[\text{C}_{14}\text{H}_{10}\text{N}_2\text{O}_2]$, 99.99%, Sigma Aldrich, CAS no. 1758-68-5) and 0.1 M lithium perchlorate ($[\text{LiClO}_4]$ (99.9%, Sigma Aldrich, CAS No. 7791-03-9) in a solution of acetonitrile ($[\text{CH}_3\text{CN}]$ (99.5%, Merck Millipore, CAS No. 75-05-08)). Cyclic voltammetry was performed from 0.2 to 1.4 V at a sampling rate of 0.1 V s^{-1} for five sampling cycles (Fig. 4A). The electrode modified with poly-1,2-diaminoanthraquinone/glassy carbon (PDAAQ/GC) was then rinsed with deionized water and was ready for use.

The formed polymer showed very promising behavior for the chelation of metal cations which facilitate the formation of molybdenum oxide on its surface. Previously few reports have been published on the electrochemical determination of molybdenum oxide. Where the polymerization using a suitable electrolyte leads to an oxide layer with various oxidation states ranging from +6 to +4, where the formed molybdenum oxide electrode shows a high potential because of its high specific capacitance and good stability. The electrochemical properties of molybdenum oxide modified electrodes can be enhanced by modifying their surfaces with another active surface substances.

For the formation of molybdate oxide layer, the formed PDAAQ/GC electrode was placed in a solution of 5 mM ammonium molybdate tetrahydrate ($[(\text{NH}_4)_6\text{Mo}_7\text{O}_{24}\cdot 4\text{H}_2\text{O}]$ ($\geq 99.0\%$, Sigma Aldrich, CAS no. 12054-85-2). Where 50 mM sodium sulphate ($[\text{Na}_2\text{SO}_4]$ (9.5–100.5%, Merck Millipore, CAS no. 7757-82-6) was added with a pH of 3 adjusted with sulfuric acid ($[\text{H}_2\text{SO}_4]$ (98%, Merck Millipore, CAS No. 7664-93-9). Cyclic voltammetry in the potential range of -0.8 to 0.2 V at a sampling rate of 50 mV/S for 10 sampling cycles, obtaining the voltammogram as shown in Fig. 4B. Then, the prepared mixed (Mo_xO_y /PDAAQ/GC) modified electrode was washed with deionized water and was ready for phosphate determination.

Orthophosphate stock solutions with a concentration of 10 mM were prepared from di-potassium hydrogen phosphate ($[\text{KH}_2\text{PO}_4]$ (99.5–100.5%, Merck Millipore, CAS No. 7778-77-0). Artificial seawater was prepared at a concentration of 34.5 g/L sodium chloride ($[\text{NaCl}]$ (99.5–100.5%, Merck Millipore, CAS No. 7647-14-5).

Square wave voltammetry (SWV) was used for the electrochemical determination of orthophosphate in seawater (34.5 g/L). SWV was selected because of its unique properties of suppressing the charging current and increasing the faradic current. It is a technique that uses a combination of square wave and stair-step potential ramp. The current is sampled twice in this technique, at the beginning of the pulse and at the end of the pulse, to reduce the influence of the capacitance current. The measurement has been done under acidic conditions into a solution of 2.5 M Sulfuric acid to achieve a pH of less than 1 to exclude the possible interferent of orthosilicate. Orthosilicate ion (SiO_4^{4-}) is the most common interferent for determination of phosphate by molybdate. It has the same tendency as orthophosphate to react with molybdate and form the silicomolybdate complex. One possible to exclude the interfering from silicate, it is performing the determination of orthophosphate at high acidic conditions at pH less than 1¹⁹.

Orthophosphate was determined by square-wave voltammetry in a solution of artificial seawater with a pH 1 adjusted with concentrated sulfuric acid with a potential range of -0.2 to 0.4 V with a step potential of 1 mV, amplitude of 25 mV, and frequency of 100 mV.

Measurements on real seawater samples were performed with an ultraviolet spectrophotometer (UV) from Hach using the classic blue phosphomolybdate complex.

Data availability

All the data are reported within the manuscript.

Received: 29 April 2023; Accepted: 10 August 2023

Published online: 21 August 2023

References

1. Foster, B. L. *et al.* Phosphate: Known and potential roles during development and regeneration of teeth and supporting structures. *Birth Defects Res. C. Embryo Today* **84**, 281–314. <https://doi.org/10.1002/bdrc.20136> (2008).
2. Kolodiazny, O. I. Phosphorus compounds of natural origin: Prebiotic, stereochemistry, application. *Symmetry* **13**, 889 (2021).
3. Savci, S. Investigation of effect of chemical fertilizers on environment. *APCBEE Proc.* **1**, 287–292. <https://doi.org/10.1016/j.apcbee.2012.03.047> (2012).
4. Azam, H. M. *et al.* Phosphorous in the environment: characteristics with distribution and effects, removal mechanisms, treatment technologies, and factors affecting recovery as minerals in natural and engineered systems. *Environ. Sci. Pollut. Res.* **26**, 20183–20207 (2019).
5. Carpenter, S. R. Eutrophication of aquatic ecosystems: bistability and soil phosphorus. *Proc. Natl. Acad. Sci. USA* **102**, 10002–10005. <https://doi.org/10.1073/pnas.0503959102> (2005).

6. Fukumoto, S. Phosphate metabolism and vitamin D. *BoneKey Rep.* **3**, 25 (2014).
7. Rice, E. W., Bridgewater, L. & Association, A. P. H. *Standard Methods for the Examination of Water and Wastewater* Vol. 10 (American Public Health Association, 2012).
8. Adeloju, S. B. Progress and recent advances in phosphate sensors: A review. *Talanta* **114**, 191–203 (2013).
9. Shen, X., Ju, F., Li, G. & Ma, L. Smartphone-based electrochemical potentiostat detection system using pedot: Pss/chitosan/graphene modified screen-printed electrodes for dopamine detection. *Sensors* **20**, 2781 (2020).
10. Bralić, M., Prkić, A., Radić, J. & Pleslić, I. Preparation of phosphate ion-selective membrane based on silver salts mixed with PTFE or carbon nanotubes. *Int. J. Electrochem. Sci.* **13**, 1390–1399 (2018).
11. Sasaki, S., Ozawa, S., Citterio, D., Yamada, K. & Suzuki, K. Organic tin compounds combined with anionic additives—an ionophore system leading to a phosphate ion-selective electrode?. *Talanta* **63**, 131–134 (2004).
12. Zeitoun, R. & Biswas, A. Potentiometric determination of phosphate using cobalt: A review. *J. Electrochem. Soc.* **167**, 127507 (2020).
13. Sivasankaran, U. *et al.* Ultrasensitive electrochemical sensing of phosphate in water mediated by a dipicolylamine-zinc(II) complex. *Sens. Actuators B Chem.* **321**, 128474. <https://doi.org/10.1016/j.snb.2020.128474> (2020).
14. Huang, Y. An all-solid-state phosphate electrode with H₃PO₄ doped polyaniline as the sensitive layer. *Int. J. Electrochem. Sci.* <https://doi.org/10.20964/2017.06.18> (2017).
15. Satoh, H. *et al.* Improvement of a phosphate ion-selective microsensor using bis (dibromophenylstannyl) methane as a carrier. *Anal. Sci.* **33**, 825–830 (2017).
16. Cinti, S., Talarico, D., Palleschi, G., Moscone, D. & Arduini, F. Novel reagentless paper-based screen-printed electrochemical sensor to detect phosphate. *Anal. Chim. Acta* **919**, 78–84. <https://doi.org/10.1016/j.aca.2016.03.011> (2016).
17. Jońca, J. *et al.* Reagentless and silicate interference free electrochemical phosphate determination in seawater. *Electrochim. Acta* **88**, 165–169. <https://doi.org/10.1016/j.electacta.2012.10.012> (2013).
18. Barus, C., Romanytsia, I., Striebig, N. & Garçon, V. Toward an in situ phosphate sensor in seawater using square wave voltammetry. *Talanta* **160**, 417–424. <https://doi.org/10.1016/j.talanta.2016.07.057> (2016).
19. Altahan, M. F., Achterberg, E. P., Ali, A. G. & Abdel-Azzem, M. NaOH pretreated molybdate-carbon paste electrode for the determination of phosphate in seawater by square wave voltammetry with impedimetric evaluation. *J. Electrochem. Soc.* **168**, 127503 (2021).
20. Altahan, M. F., Esposito, M., Bogner, B. & Achterberg, E. P. The use of bi-potentiostat as a simple and accurate electrochemical approach for the determination of orthophosphate in seawater. *Sensors* **23**, 2123 (2023).
21. Tian, L., Liu, L., Chen, L., Lu, N. & Xu, H. Fabrication of amorphous mixed-valent molybdenum oxide film electrode deposited on a glassy carbon electrode and its application as an electrochemistry sensor of iodate. *Sens. Actuators B Chem.* **105**, 484–489 (2005).
22. Hassan, K. M., Gaber, S. E., Altahan, M. F. & Azzem, M. A. Novel sensor based on poly (1, 2-diaminoanthraquinone) for individual and simultaneous anodic stripping voltammetry of Cd²⁺, Pb²⁺, Cu²⁺ and Hg²⁺. *Electroanalysis* **30**, 1155–1162 (2018).
23. Hassan, K. M., Gaber, S. E., Altahan, M. F. & Azzem, M. A. Single and simultaneous voltammetric sensing of lead (II), cadmium (II) and zinc (II) using a bimetallic Hg-Bi supported on poly (1, 2-diaminoanthraquinone)/glassy carbon modified electrode. *Sens. Bio-Sens. Res.* **29**, 100369 (2020).
24. Ali, A. G., Altahan, M. F., Beltagi, A. M., Hathoot, A. A. & Abdel-Azzem, M. Voltammetric and impedimetric determinations of selenium (iv) by an innovative gold-free poly (1-aminoanthraquinone)/multiwall carbon nanotube-modified carbon paste electrode. *RSC Adv.* **12**, 4988–5000 (2022).
25. Altahan, M. F., Ali, A. G., Hathoot, A. A. & Abdel-Azzem, M. Ultrasensitive platform for electrochemical sensing of copper and antimony based on poly (1, 5-diaminoanthraquinone)/multiwalled carbon nanotubes/carbon paste electrode. *J. Electrochem. Soc.* **167**, 127510 (2020).
26. Altahan, M. F., Esposito, M. & Achterberg, E. P. Improvement of on-site sensor for simultaneous determination of phosphate, silicic acid, nitrate plus nitrite in seawater. *Sensors* **22**, 3479 (2022).
27. Li, Y., Jiang, T., Yu, X. & Yang, H. Phosphate sensor using molybdenum. *J. Electrochem. Soc.* **163**, B479 (2016).
28. Topcu, C. *et al.* Structural characterization of chitosan-smectite nanocomposite and its application in the development of a novel potentiometric monohydrogen phosphate-selective sensor. *Mater. Res. Bull.* **98**, 288–299. <https://doi.org/10.1016/j.materresbull.2017.09.068> (2018).
29. Abbas, M. N., Radwan, A. L. A., Nooredeen, N. M. & El-Ghaffar, M. A. A. Selective phosphate sensing using copper monoamino-phthalocyanine functionalized acrylate polymer-based solid-state electrode for FIA of environmental waters. *J. Solid State Electrochem.* **20**, 1599–1612 (2016).
30. Talarico, D., Arduini, F., Amine, A., Moscone, D. & Palleschi, G. Screen-printed electrode modified with carbon black nanoparticles for phosphate detection by measuring the electroactive phosphomolybdate complex. *Talanta* **141**, 267–272. <https://doi.org/10.1016/j.talanta.2015.04.006> (2015).
31. Ogabiela, E., Adeloju, S. B., Cui, J., Wu, Y. & Chen, W. A novel ultrasensitive phosphate amperometric nanobiosensor based on the integration of pyruvate oxidase with highly ordered gold nanowires array. *Biosens. Bioelectron.* **71**, 278–285. <https://doi.org/10.1016/j.bios.2015.04.026> (2015).
32. Cui, J. *et al.* Electrochemical biosensor based on Pt/Au alloy nanowire arrays for phosphate detection. *J. Electrochem. Soc.* **162**, B62–B67. <https://doi.org/10.1149/2.0701503jes> (2014).
33. Xu, K., Kitazumi, Y., Kano, K. & Shirai, O. Phosphate ion sensor using a cobalt phosphate coated cobalt electrode. *Electrochim. Acta* **282**, 242–246 (2018).
34. van den Hoop, M. A. & van Staden, J. J. Determination of phosphate in natural waters by capillary electrophoresis Influence of solution composition on migration time and response. *J. Chromatogr. A* **770**, 321–328 (1997).
35. Pessoa-Neto, O. D., Silva, T. A., dos Santos, V. B. & Fatibello-Filho, O. A compact microcontrolled microfluidic system for photometric determination of phosphate in natural water samples. *Aust. J. Chem.* **68**, 1108–1114 (2015).
36. Clinton-Bailey, G. S. *et al.* A lab-on-chip analyzer for in situ measurement of soluble reactive phosphate: improved phosphate blue assay and application to fluvial monitoring. *Environ. Sci. Technol.* **51**, 9989–9995 (2017).
37. Legiret, F.-E. *et al.* A high performance microfluidic analyser for phosphate measurements in marine waters using the vanadomolybdate method. *Talanta* **116**, 382–387 (2013).
38. Wang, R., Wang, N., Ye, M. & Zhu, Y. Determination of low-level anions in seawater by ion chromatography with cycling-column-switching. *J. Chromatogr. A* **1265**, 186–190 (2012).
39. KANSO TECHNOS CO., L. *Certificate of Analysis Certified Reference Material KANSO CRM Lot.CG*. [https://www.jamstec.go.jp/scor/doc/certificate_\(CG\)_Sample.pdf](https://www.jamstec.go.jp/scor/doc/certificate_(CG)_Sample.pdf). Accessed March 2023.
40. KANSO TECHNOS CO., L. *Certificate of Analysis Certified Reference Material KANSO CRM Lot.CI*. http://www.kanso.co.jp/eng/pdf/certificate_ci.pdf. Accessed March 2023.
41. KANSO TECHNOS CO., L. *Certificate of Analysis-Certified Reference Material KANSO CRM Lot.CH*. http://www.kanso.co.jp/eng/pdf/certificate_ch.pdf. Accessed March 2023.

Acknowledgements

Authors would like to thank the Alexander von Humboldt Foundation for the scientific donation of some electrochemical measurement apparatus.

Author contributions

M.F.A. wrote the main manuscript and performed the experiments, M.A. conceived the research problem and revised the manuscript. All authors reviewed the manuscript.

Funding

Open access funding provided by The Science, Technology & Innovation Funding Authority (STDF) in cooperation with The Egyptian Knowledge Bank (EKB).

Competing interests

The authors declare no competing interests.

Additional information

Correspondence and requests for materials should be addressed to M.F.A.

Reprints and permissions information is available at www.nature.com/reprints.

Publisher's note Springer Nature remains neutral with regard to jurisdictional claims in published maps and institutional affiliations.



Open Access This article is licensed under a Creative Commons Attribution 4.0 International License, which permits use, sharing, adaptation, distribution and reproduction in any medium or format, as long as you give appropriate credit to the original author(s) and the source, provide a link to the Creative Commons licence, and indicate if changes were made. The images or other third party material in this article are included in the article's Creative Commons licence, unless indicated otherwise in a credit line to the material. If material is not included in the article's Creative Commons licence and your intended use is not permitted by statutory regulation or exceeds the permitted use, you will need to obtain permission directly from the copyright holder. To view a copy of this licence, visit <http://creativecommons.org/licenses/by/4.0/>.

© The Author(s) 2023